Journal of
Computational and Theoretical Nanoscience
Vol. 11, 1838–1843, 2014

RESEARCH ARTICLE

Structural Characterization of Deformed Boron Nitride Nanotubes

Jamal A. Talla*, Ayman Sawalha, and Hussien Sabbah

Department of Physics, King Faisal University, Al-Ahsaa-31982, Saudi Arabia

We investigated the effect of inducing deformation in individual boron nitride nanotubes by performing X-ray diffraction (XRD) simulations for different individual boron nitride nanotubes that had different geometries and were subjected to mechanical deformations. We found that the mechanical properties of boron nitride nanotubes depended sensitively on the levels of induced mechanical deformation. As a result of this dependence, mechanical deformations induced in boron nitride nanotubes caused their XRD patterns to change. We compared the XRD patterns of deformed boron nitride nanotubes with those of undeformed boron nitride nanotubes for different torsion angles.

Keywords: Boron Nitride Nanotubes, X-Ray Diffraction, Simulations, Torsion, Intensity, Incident Angle, Bragg Law.

1. INTRODUCTION

Since their discovery, boron nitride nanotubes have generated considerable interest because their hardness is comparable to that of diamonds.[1] Because the structure of boron nitride nanotubes is similar to that of carbon nanotubes,[2, 3] boron nitride nanotubes exhibit unusual mechanical properties that are similar to those of carbon nanotubes.[4–6] Contrastively, the phonon mean free path of boron nitride nanotubes is similar to that of carbon nanotubes.[6, 7] However, unlike carbon nanotubes, the electronic properties of boron nitride nanotubes are not sensitive to the chirality or diameter of the nanotube.[8] Furthermore, boron nitride nanotubes remain semiconducting materials and have an expected band gap of ~ 5 eV.[9] Moreover, depending on the required application, the band gap of a boron nitride nanotube can be controlled by covalently attaching molecules onto the nanotube side walls.[8] Furthermore, boron nitride nanotubes show a high oxidation resistance and larger low-temperature thermal conductivity as compared to carbon nanotubes.[10, 11] It is also found that the axial Young's modulus for boron nitride nanotubes is larger than that of any other known insulating nanostructure.[4] These extraordinary properties make boron nitride nanotubes a suitable candidate for several science and technology related applications. However, researchers have faced limitations and challenges in realizing the mass production of boron nitride nanotubes.[1, 2, 10, 12, 13]

Boron nitride nanotubes could undergo different structural deformations, including bending, collapsing of certain regions, or torsion.[14–16] These deformations may develop naturally during production or may be intentionally induced during processing.[17–20] Inducing such structural deformations, particularly, through the application of mechanical torsion, is an effective technique for manipulating the mechanical properties of boron nitride nanotubes.[21–24] Due to torsional deformation, the original translational symmetry and periodicity of the translational symmetry of the nanotube collapse.[21–24] Such a collapse in the symmetry mainly depends on the magnitude and direction of the applied mechanical torsion.[22] Therefore, techniques needs to be developed that would help to gain a better understanding of these types of structural deformations in boron nitride nanotubes.[25–32] The characterization-based techniques are most frequently used to understand these deformations and include transmission electron microscopy (TEM), scanning electron microscopy (SEM), neutron diffraction, and X-ray diffraction (XRD).[17–20]

Computerbased simulations of material properties have gathered interest from several researchers working in the field of computational material science. Moreover, presently, the structures of very complex molecules such as proteins, enzymes, nucleic acids, and even viruses are being investigated through the use of XRD techniques.[33–37] XRD is considered a fast, non-destructive technique for routine analysis as well as a useful and powerful technique to monitor the purification processes of raw samples.[17–20]

*Author to whom correspondence should be addressed.

1546-1955/2014/11/1838/006 doi:10.1166/jctn.2014.3576

With the help of the corresponding X-ray spectral pattern, it is possible to identify the presence of entrapped metal particles within the tubular structure of a boron nitride nanotube during the production process.[2, 9] In addition, XRD can be used to obtain structural information of disordered materials.[17–20, 38] Apart from this, the analysis of the XRD profiles of boron nitride nanotubes generates average data that describe their structural characteristics. This paper discusses the use of XRD simulations to study dislocations that might be produced in response to the mechanical torsion applied to individual single-walled boron nitride nanotubes. Our ultimate goal is to provide experimentalists with readily usable information describing the behavior and characteristics of boron nitride nanotubes subjected to torsion. Therefore, we describe in later text how the simulated diffraction patterns can be used to characterize the corresponding boron nitride nanotube samples.

2. COMPUTER SIMULATION

Commercial computer simulation software "CrystalDiffract" was used to study individual single-walled boron nitride nanotubes with different geometrical structures.[27] The CrystalDiffract algorithm first imports saved CrystalMaker software files to simulate XRD patterns through the use of easy manipulation and measurement tools and displays the patterns on a monitor. In this program, proper nanotube structures were prepared using CrystalMaker software. To simulate the nanotubes, the Cartesian coordinates of boron nitride atoms were generated for a single tube.[17] First, we transformed the original coordinates of the boron nitride graphene sheet into a new system in which the translational vector $\boldsymbol{T}$ was set along the y-axis.[18] Next, cylindrical transformation was used to convert the boron nitride graphene atomic coordinates (x, y) into those of the nanotube (X, Y, Z).[19, 20] Then, suitable torsion was applied by inclining the translational vector in the expanded plane. Applying torsion is advantageous compared to the translational unit-cell method because it does not cause the number of boron nitride atoms per unit cell to change.[19, 20] The simulated nanotube structures were then imported into the CrystalDiffract program.

The raw data were collected by making a short-wavelength X-ray beam incident on the samples. Analysis of the X-ray scattering reveals various aspects of the atomic structure. Background correction is performed by removing the $k\alpha_2$ peaks before identifying the diffraction

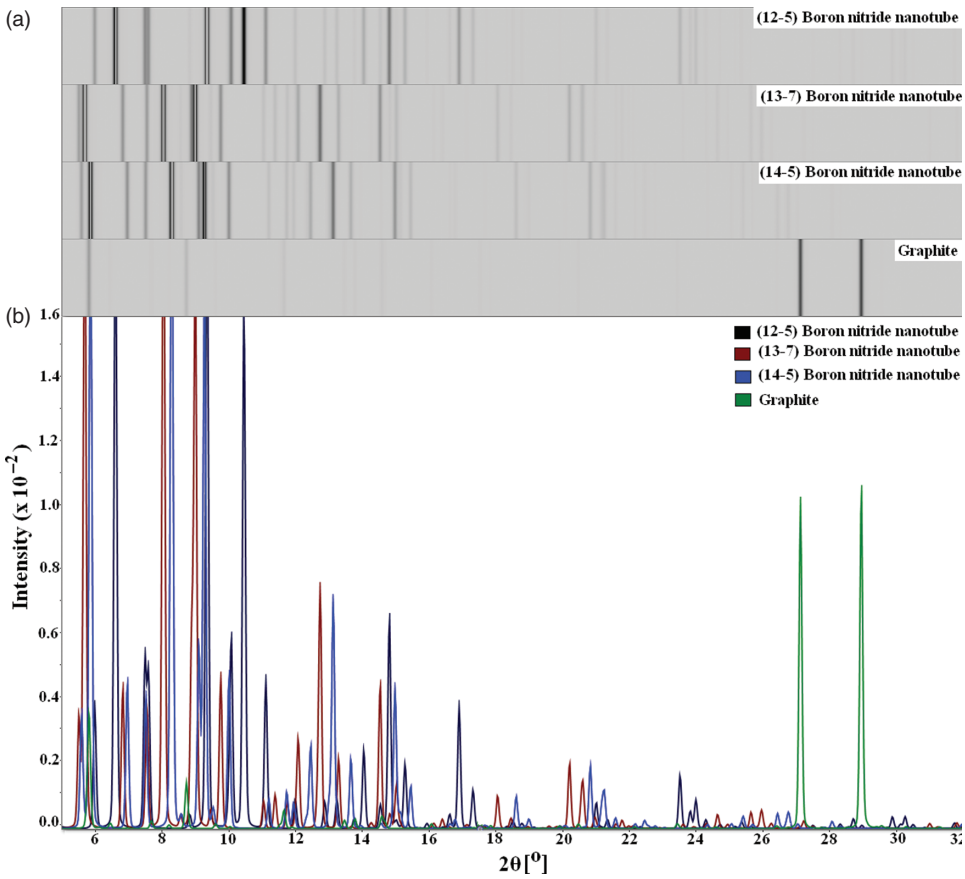

Fig. 1. (a) Film representation shows a Comparison of the peaks intensity for graphite and different geometrical structures of individual boron nitride nanotube. (b) Peak comparison of simulated XRD profiles for graphite and different geometrical structures of individual boron nitride nanotubes.

peaks.[27] The peak profiles were exported, and the final results were properly represented as a 2-dimensional image of 2θ and the intensity. The results of the simulation were compared, for certain pristine boron nitride nanotubes, with the XRD profiles of graphite.[17]

3. DISCUSSION AND ANALYSIS

When mechanical torsion is applied along the tube axes, it is expected to induce several structural deformations. Therefore, understanding the effect of applying torsion to a boron nitride nanotube is necessary, because the distortions produced on account of the mechanical torsion applied to the tubes have a significant influence on their mechanical properties. The exact effect of applying mechanical torsion on the nanotube properties has been ignored in most theoretical studies and remains an unaddressed topic; it requires further investigation. To study the mechanism that produces the mechanical torsion, we simulated the response of individual single-walled boron nitride nanotube samples having different chiralities [(12, 5), (13, 7), and (14, 5)] when mechanical torsion was applied, by using XRD. A short wavelength ($\lambda = 1$ Å) was used in order to negate the effects of multiple scattering, absorption, and polarization. We found that the main characteristics of the profiles of boron nitride nanotubes closely resemble those of graphite owing to the intrinsic nature of both these nanotubes (Figs. 1(a) and (b)). The (h k 0) peaks exhibit an asymmetric shape owing to the curvature of the boron nitride nanotube. This asymmetric shape of the (h k 0) peaks was ascribed to the fact that boron nitride sheets were rolled to form a nanotube. The orientation of the boron nitride nanotube relative to the incident X-ray beam and the lattice distortion produced by the applied torsion are important factors that determine the width and intensity of the (1 1 0) interlayer peak (see Figs. 2–4).

In all the samples, different structural deformations occurred upon the application of torsion. For example, for the same peak, a sharp increase in the intensity was accompanied by a slight reduction in 2θ, whereas a shift toward a lower angle was consistent with the surface curvature. However, in other regions, the peak intensity showed a relatively small decrease. For instance, at $2\theta = 14.5°$, when torsion was applied to the nanotube samples (40°/Å), the intensity was increased and the full width at half-maximum (FWHM) became narrowed (see Fig. 2(b)). This behavior was also observed to occur in all the remaining boron nitride nanotube samples (see Figs. 3 and 4). However, for the (12, 5) nanotube sample, at $2\theta = 21.0°$,

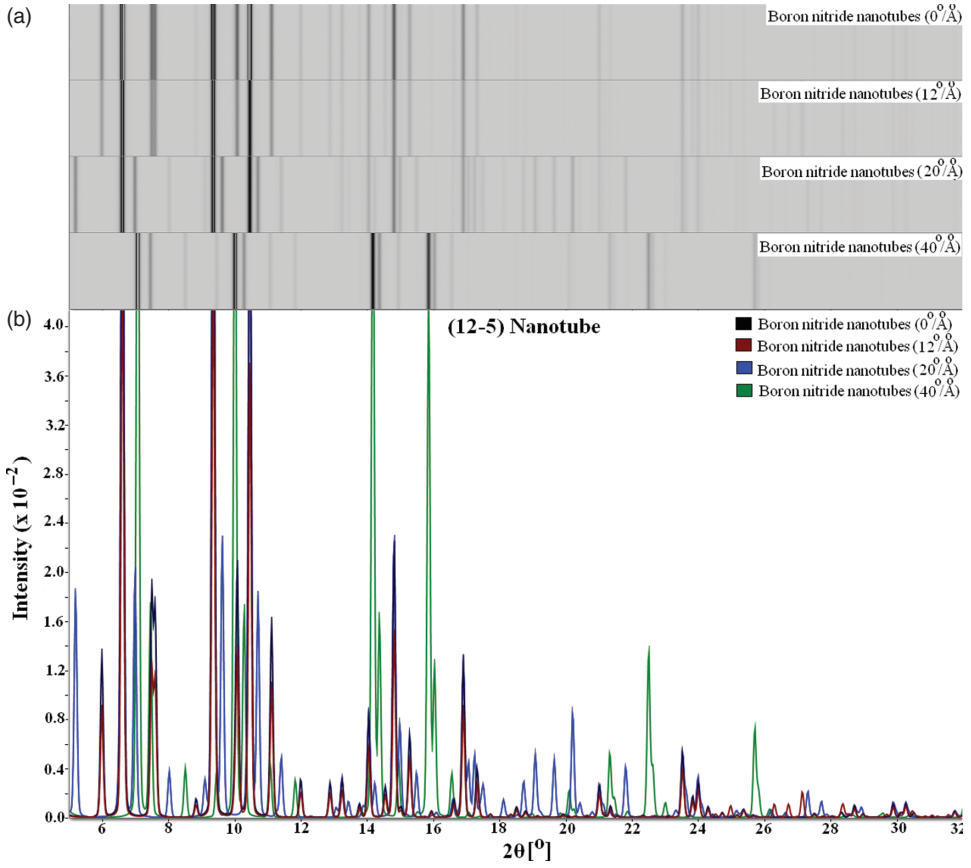

Fig. 2. (a) Simulated XRD profiles as film representation shows a comparison of the peaks intensity for deformed and undeformed (12, 5) boron nitride nanotube at different torsional angles. (b) A peak comparison of the simulated XRD profiles for deformed and undeformed (12, 5) nanotubes samples. A change in 2θ as a function of the intensity occurs when the nanotubes samples were deformed.

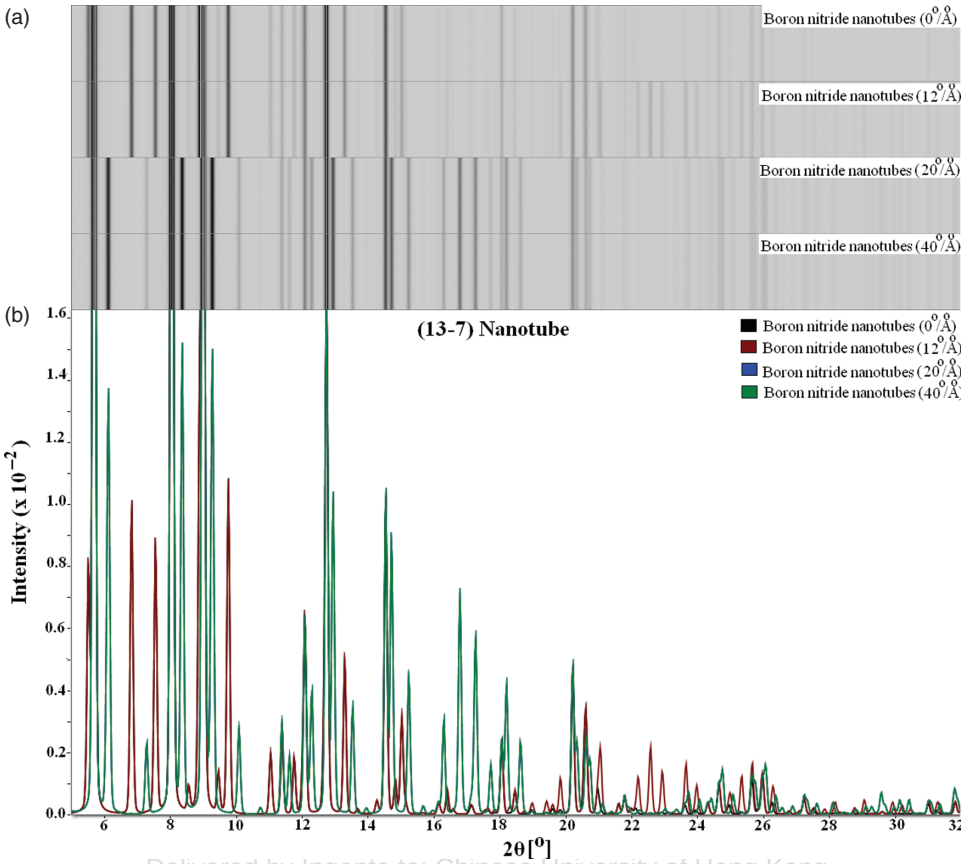

Fig. 3. (a) Simulated XRD profiles as film representation shows a comparison of the peaks intensity for deformed and undeformed (13, 7) boron nitride nanotube at different torsional angles. (b) A peak comparison of the simulated XRD profiles for deformed and undeformed (13, 7) nanotubes samples. A change in 2θ as a function of the intensity occurs when the nanotubes samples were deformed.

the applied mechanical torsion produced a sharp decrease in the intensity accompanied by an increase in 2θ, (see Fig. 2). This sudden decrease in the intensity could be correlated with the complete collapse of the symmetry of the nanotubes to which mechanical torsion was applied. Moreover, the increase to higher angles could be correlated to the deformation of the surface curvature, induced by the applied mechanical torsion. For the (14, 5) pure boron nitride nanotubes, clear informative signals were predicted in the 18°–22° range (see Fig. 4). In this region, the nanotubes exhibited a weak broad peak centered at $\sim$18.6°. This could be attributed to the (0 0 1) interlayer peak of graphite, which appeared at $\sim$45.0°. Other typical signals for the (14, 5) pure nanotubes were the intense peaks appearing at $\sim$20.86° and a less intense peak appearing at $\sim$21.24° (Fig. 4). These reflections are ascribed to the (0 5 0) and (5 5 0) crystallographic planes, respectively. The width of these reflections needs to be carefully considered, particularly when it is compared to that in the case of graphite. In addition, large mechanical torsion has a direct influence not only on the Bragg angle but also on the peak intensity. This behavior could be ascribed to the curvature effect (see Figs. 2–4). Moreover, for the same nanotube sample to which mechanical torsion was applied, some peaks appeared while others disappeared. For example, in the (13, 7) torsion nanotube sample (40°/Å), specifically, in the 15°–18° region, clear, sharp peaks appeared, whereas for the pure sample, the intensity of the peaks weakened or the peaks nearly disappeared. Conversely, in the 20°–24° regions, a clear peak appeared for the pure sample and clearly disappeared in the sample to which mechanical torsion was applied (40°/Å), (see Figs. 3(a) and (b)). The appearance of the strong first-order peak at about $2\theta = 4°$ was a good indicator of a nanotube rope lattice; this strong peak is known to generally be followed by series of weaker peaks for 2θ in the range of 10°–32°.

Furthermore, for the same sample, other typical reflections set at about 30.4° and a lower one at $2\theta = 32.0°$ peak positions. Finally, the application of mechanical torsion directly influences the (2 0 0) peaks in all nanotube samples, and valuable information can be attained from the analysis of the intensity of the (2 0 0) diffraction peak. For instance, in (12, 5), the peak weakened and broadened in a region having a low diffraction angle ($2\theta = 12.4°$), as shown in Figures 2(a) and (b). However, the line shape of the (2 0 0) peaks was broadened and its intensity was weakened in the region of a low diffraction angle when mechanical torsion was applied to the nanotube.

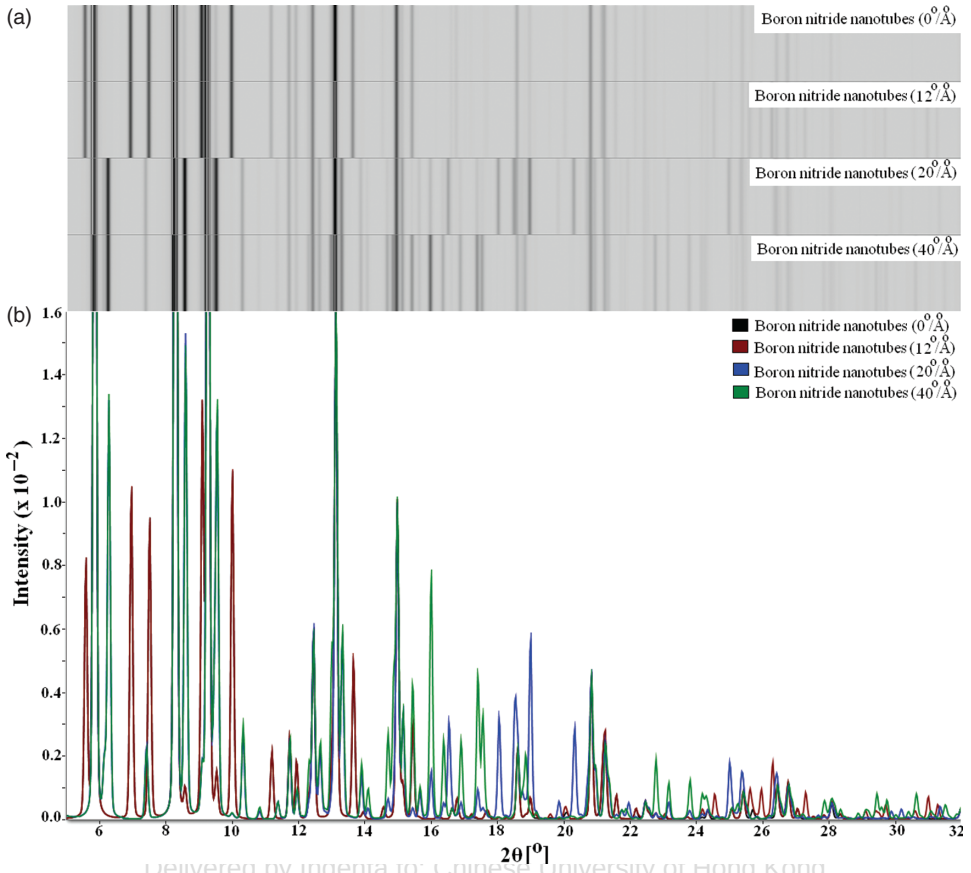

Fig. 4. (a) Simulated XRD profiles as film representation shows a comparison of the peaks intensity for deformed and undeformed (14, 5) boron nitride nanotube at different torsional angles. (b) A peak comparison of the simulated XRD profiles for deformed and undeformed (14, 5) nanotubes samples. A change in 2θ as a function of the intensity occurs when the nanotubes samples were deformed.

4. CONCLUSION

In this work, XRD patterns were simulated to study the effects of mechanical deformations induced in boron nitride nanotube samples in order to predict the structural modifications that the samples would experience due to the applied mechanical torsion. XRD profiles were simulated for different geometrical structures of individual boron nitride nanotube samples. For all the samples, one peak showed a sharp increase in intensity along with a slight reduction in 2θ, although in other regions, the peak intensity decreased slightly. We found that in some regions, mechanical torsion produced a sharp decrease in the intensity and an increase in 2θ. We attributed this sudden decrease in the intensity to the complete collapse of symmetry in the nanotubes subjected to torsion. The same reason was considered to cause the increase to higher torsional angles, in regions other than those where deformation occurred in the surface curvature as a result of the applied mechanical torsion. Furthermore, increased mechanical torsion directly influenced not only the intensity of the peaks but also the Bragg angle; we correlated this observation to the curvature effect. Moreover, for the same nanotube sample to which mechanical torsion was applied, some peaks appeared while others disappeared. Finally, the applied mechanical torsion directly affected the (2 0 0) peaks in all nanotube samples. In particular, when mechanical torsion was applied, the line shape of the (2 0 0) peaks was broadened, its intensity was weakened, and a corresponding reduction occurred in the diffraction angle.

Acknowledgments: The author gratefully acknowledges the Scientific Research Deanship at King Faisal University (#140007) for financial support.

References

1. C. Zhi, Y. Bando, C. Tang, and D. Golberg, *Mater. Sci. Eng.: R: Reports* 70, 92 (**2010**).
2. M. Terrones, J. M. Romo-Herrera, E. Cruz-Silva, F. Lpez-UrÃas, E. MuÃoz-Sandoval, J. J. Velzquez-Salazar, H. Terrones, Y. Bando, and D. Golberg, *Mater. Today* 10, 30 (**2007**).
3. B. Tüzün and C. Erkoç, *Quantum Matter* 1, 136 (**2012**).
4. D. V. Fakhrabad and N. Shahtahmassebi, *Mater. Chem. Phys.* (**2013**).
5. A. Rochefort and P. Avouris, *Phys. Rev. B* 60, R16338 (**1999**).
6. P. A. G. Sankar and K. U. Kumar, *European Journal of Scientific Research* 60, 324 (**2011**).

7. K. Kiani, H. Ghaffari, and B. Mehri, *Current Applied Physics* 13, 107 **(2013)**.
8. R. Chegel and S. Behzad, *J. Phys. Chem. Solids* 73, 154 **(2012)**.
9. J.-F. Jia, H.-S. Wu, and H. Jiao, *Physica B: Condens. Matter* 381, 90 **(2006)**.
10. H. Aoki, H. Shima, C. Kimura, and T. Sugino, *Diamond Relat. Mater.* 16, 1300 **(2007)**.
11. J. Li, H. Lin, Y. Chen, Q. Su, and Q. Huang, *Chem. Eng. J.* 174, 687 **(2011)**.
12. Y. Chen, Z. Tong, and L. Luo, *Chin. J. Chem. Eng.* 16, 485 **(2008)**.
13. J. Wang, H. Li, Y. Li, H. Yu, Y. He, and X. Song, *Physica E: Low-Dimensional Systems and Nanostructures* 44 **(2011)**.
14. Y.-Q. Xu, A. Barnard, and P. L. McEuen, *Nano Lett.* 9, 1609 **(2009)**.
15. K. Kato, T. Koretsune, and S. Saito, *Journal of Physics: Conference Series* 302, 012007 **(2011)**.
16. S.-C. Her and T.-Y. Shiu, *J. Comput. Theor. Nanosci.* 9, 1741 **(2012)**.
17. J. A. Talla, *Nanosci. Nanotechnol. Lett.* 5, 568 **(2013)**.
18. J. A. Talla, *J. Comput. Theor. Nanosci.* 10, 1963 **(2013)**.
19. J. A. Talla, A. Al-Sharif, A. Al-Jaafari, and A. H. Sabbah, *J. Comput. Theor. Nanosci.* 10, 2631 **(2012)**.
20. J. A. Talla, *J. Comput. Theor. Nanosci.* 10, 1963 **(2013)**.
21. M. Mirnezhad, R. Ansari, and H. Rouhi, *Superlattices Microstruct.* 53, 223 **(2013)**.
22. S.-Y. Wu, Y.-L. Huang, C.-C.M. Ma, S.-M. Yuen, C.-C. Teng, S.-Y. Yang, *Composites Part A* 42 **(2011)**.
23. E. Barraud, S. Begin-Colin, G. Le Car, O. Barres, and F. Villieras, *J. Alloys Compd.* 456, 224 **(2008)**.
24. C. Suryanarayana and N. Al-Aqeeli, *Prog. Mater Sci.* 58, 383 **(2013)**.
25. J. Cambedouzou, M. Chorro, R. Almairac, L. NoÃ©, E. Flahaut, S. Rols, M. Monthioux, and P. Launois, *Physical Review B-Condensed Matter and Materials Physics* 79, 195423 **(2009)**.
26. P. Coquay, R. E. Vandenberghe, E. De Grave, A. Fonseca, P. Piedigrosso, and J. B. Nagy, *J. Appl. Phys.* 92, 1286 **(2002)**.
27. J. Oddershede, K. Nielsen, and K. Stahl, *Zeitschrift fur Kristallographie* 222, 186 **(2007)**.
28. J. Chancolon, F. Archaimbault, S. Bonnamy, A. Traverse, L. Olivi, and G. Vlaic, *J. Non-Cryst. Solids* 352, 99 **(2006)**.
29. J. Talla, D. Zhang, M. Kandadai, A. Avadhanula, and S. Curran, *Physica B: Condensed Matter* 405, 4570 **(2010)**.
30. S. A. Curran, J. A. Talla, D. Zhang, and D. L. Carroll, *J. Mater. Res.* 20, 3368 **(2005)**.
31. T. Ono, Y. Fujimoto, and S. Tsukamoto, *Quantum Matter* 1, 4 **(2012)**.
32. P. K. Bose, N. Paitya, S. Bhattacharya, D. S. De, K. M. Chatterjee, S. Pahari, and K. P. Ghatak, *Quantum Matter* 1, 89 **(2012)**.
33. D. Reznik, C. H. Olk, D. A. Neumann, and J. R. D. Copley, *Phys. Rev. B* 52, 116 **(1995)**.
34. A. Cao, C. Xu, J. Liang, D. Wu, and B. Wei, *Chem. Phys. Lett.* 344, 13 **(2001)**.
35. A. Cao, C. Xu, J. Liang, D. Wu, and B. Wei, *Chem. Phys. Lett.* 344, 13 **(2001)**.
36. D. Rende, L. Ozgur, N. Baysal, and R. Ozisik, *J. Comput. Theor. Nanosci.* 9, 1658 **(2012)**.
37. B. K. Agrawal, P. S. Yadav, and R. K. Yadav, *J. Comput. Theor. Nanosci.* 9, 1830 **(2012)**.
38. Y. Li and H. Li, *J. Mater. Sci. Technol.* 26, 542 **(2010)**.

Received: 29 June 2013. Accepted: 20 July 2013.